

## Determination of the momentum of impulsively generated phonon polaritons

János Hebling

University of Pécs, Department of Experimental Physics, H-7624 Pécs, Hungary

(Received 20 September 2001; published 14 February 2002)

It is proved experimentally that the momentum of phonon polaritons generated by impulsive excitation has to be calculated using the same formula as for the case of long-pulse coherent anti-Stokes Raman scattering experiments. Attention is also drawn to the fact that, contrary to the common belief, the generated phonon polaritons are not exactly counterpropagating.

DOI: 10.1103/PhysRevB.65.092301

PACS number(s): 78.47.+p, 71.36.+c, 63.20.-e

Coherent anti-Stokes Raman scattering (CARS) has been used for a long time for investigation of the dynamics of Raman-active lattice and molecular vibrations. In the CARS experiment two light beams having frequency of  $\omega_L$  and  $\omega_S$  crossing each other at an angle of  $\Theta$  are used to excite vibrations having a frequency of

$$\Omega = \omega_L - \omega_S. \quad (1)$$

It is well established that the  $\mathbf{q}$  wave vector of the generated vibration (phonon) is determined by the crossing angle  $\Theta$  and the  $\mathbf{k}_L$  and  $\mathbf{k}_S$  wave vectors of the two beams according to the vector diagram depicted in Fig. 1(a). Since the wave vectors multiplied by  $\hbar$  give the vector of momentum, the vector diagram expresses the momentum conservation principle. According to the figure, the magnitude of  $\mathbf{q}$  is given as

$$q = \sqrt{k_L^2 + k_S^2 - 2k_L k_S \cos(\Theta)}. \quad (2)$$

In the middle of the 1980s the pulse duration available from lasers became much shorter than the phonon oscillation period in most semiconductors and dielectrics. In the spectral domain this means that their spectrum contains significant components with a separation equal to typical phonon frequencies. This makes it possible to excite phonons impulsively by crossing two beams split from the same beam. In the impulsive stimulated Raman scattering (ISRS) experiments<sup>1</sup> the scattering of photons of a delayed beam is detected in order to follow the decay of the excited vibrations.

Since impulsive excitation is applied there is an uncertainty in the literature about how the wave vector (or mo-

mentum) of the excited phonon is determined by the crossing angle and the wave vector of the exciting beams. Most groups<sup>1-4</sup> use the following formula:

$$q = \frac{4\pi \sin(\Theta_o/2)}{\lambda_c} = 2k_c \sin(\Theta_i/2), \quad (3)$$

where  $\Theta_o$  and  $\Theta_i$  are the crossing angle of the two beams outside and inside the investigated material, respectively,  $\lambda_c$  is the central wavelength, and  $k_c = 2\pi n/\lambda_c$  is the magnitude of the wave vector inside the material having an index of refraction of  $n$ . Using this formula, Ref. 5 is usually cited, where  $q$  is given as the magnitude of the grating vector in laser-induced dynamic gratings.

Another group used Eq. (2) in their first ISRS experiments.<sup>6,7</sup> Later they argued<sup>8</sup> that Eq. (3) has to be used to calculate the wave vector of phonons generated in ISRS experiments, since the two crossing beams have the same central frequency and play an equivalent role in the excitation of phonons. Drawings similar to Fig. 1(b) are usually given<sup>8,3</sup> in order to display this equivalent role of the beams. Using the double arrow for the indication of the created phonon expresses the idea that counterpropagating phonons are excited. Recently the same group proposed<sup>9</sup> such equations for the  $q$  vector of phonons generated by ISRS in anisotropic materials, which is equivalent to Eq. (2) for the isotropic case. However, they did not conclude that Eq. (2) has to be used for the isotropic case as well, and they published drawings suggesting that counterpropagating phonons are created. It seems that the application of Eq. (3) and belief in counterpropagating phonons remained common<sup>10</sup> in the ISRS literature.

The aim of this paper is to demonstrate experimentally that Eq. (2) gives the right magnitude of the momentum of phonons created in ISRS experiments and the drawing of Fig. 1(a) gives the right direction of the phonons. This conclusion should follow simply from the conservation of momentum and energy for the quantum process of Raman scattering [the process illustrated in Fig. 1(b) does not satisfy conservation of energy]. However, an experimental demonstration seems to be useful because of the above-indicated confusion. Besides the obvious fundamental significance, it is important to point out what the right formula is because ISRS experiments are used<sup>2-4,8,10</sup> to determine the dispersion curve of phonon polaritons and the application of a wrong formula naturally results in inaccurate dispersion curves.

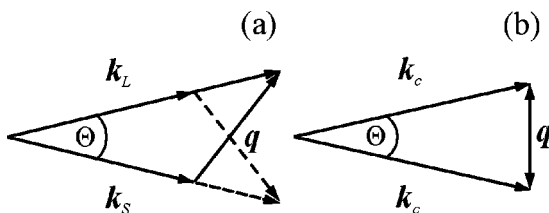


FIG. 1. Wave vector diagram of phonon generation (a) by long pulses (see only arrows with solid lines) and (b) by impulsive excitation according to the literature. (a) including both solid and dashed arrows depicts the wave vector diagram of phonon generation by impulsive excitation in accordance to the present observations.

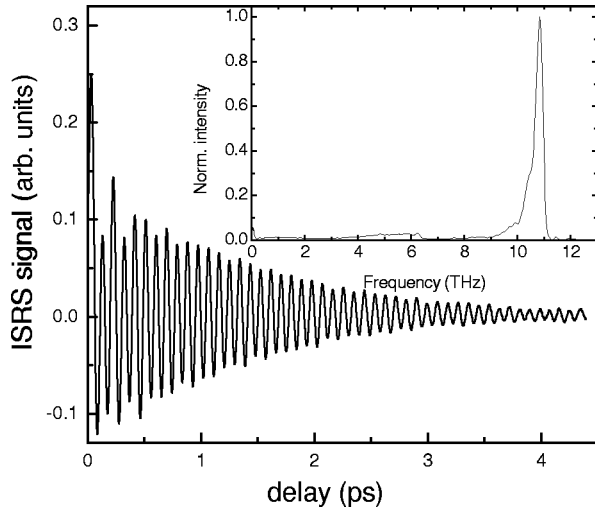


FIG. 2. ISRS trace (diffracted intensity vs delay of the probe pulse) measured for  $\Theta = 15.4^\circ$  angle of intersection of the pump beams and its Fourier transform (inset).

In order to be able to decide between Eqs. (2) and (3) we performed an ISRS experiment to measure the dispersion of phonon polaritons excited in GaP. GaP was chosen since its dispersion is well known<sup>11</sup> and the  $q$  values calculated according to Eqs. (2) and (3) differ strongly because of the relatively high ( $\Omega = 367 \text{ cm}^{-1}$ ) TO phonon frequency. Light pulses of a Ti:s laser having 25 fs pulse duration and 810 nm central wavelength were used as the two pump and probe pulses. A spherical lens focused the corresponding three beams. A transmission boxcar geometry was applied; that is, the three light spots on the lens were situated at the three corners of a rectangle. Before the incidence on the focusing lens the probe beam was reflected on a shaker, which introduced a scanned delay. The probe beam diffracted (scattered) on the transient grating (phonon polariton) created by the two pump beams was detected by a photodiode. Its signal was fed into a computer through a fast analog-to-digital (AD) converter, and the averaged signal was recorded. Phonon polaritons were excited impulsively in a slightly wedged ( $10^\circ$ ) high-purity ( $< 3 \times 10^{-15} \text{ cm}^{-3}$ ) GaP sample having a  $\langle 110 \rangle$  front surface. The electric field of the pump and probe beams was set along the  $[111]$  and  $[112]$  direction of the GaP sample. For this orientation strong TO phonon-polariton signal is expected, while LO phonon generation is not allowed.

The  $\Theta_o$  crossing angle of the pump beams was set by adjusting the  $b$  separation of the beam spots on the focusing lens and it was calculated according to

$$\Theta_o = 2 \tan^{-1} \left( \frac{b}{2f} \right). \quad (4)$$

The ISRS traces measured for  $\Theta_o = 15.4^\circ$  are displayed in Fig. 2. The original signal consists of a strong peak at zero delay, because of the electronic Kerr nonlinearity of GaP. This peak is followed by a long-living background (attributed to refractive index grating created by the two excitation beams via two-photon absorption) weakly modulated on top

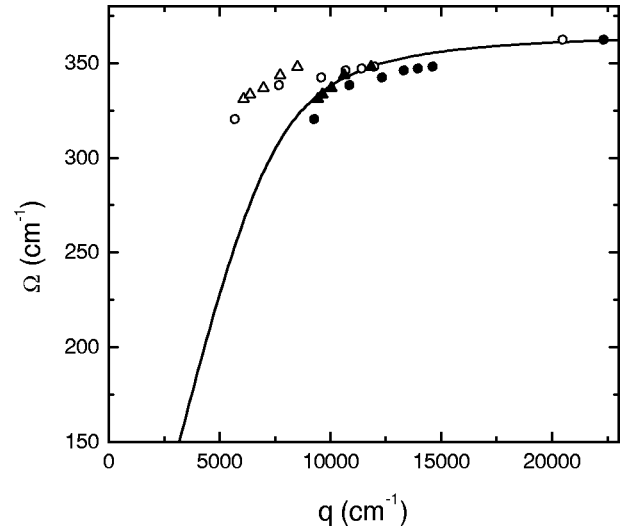


FIG. 3. Measured frequency of polariton in GaP vs the wave vector calculated according to Eq. (2) (solid symbols) and Eq. (3) (open symbols), respectively. Circles and triangles are for measured values using  $f = 100 \text{ mm}$  and  $f = 200 \text{ mm}$  focal length lenses, respectively. The solid line is the theoretical dispersion curve of the TO phonon polariton in GaP calculated according to Eq. (5)

by the coherent phonon oscillations. Figure 2 depicts the temporal evolution of only the modulated part of the signal. The inset of Fig. 2 shows the spectrum of the oscillations obtained by Fourier transformation of the time domain trace. The sharp peak at 10.9 THz ( $363 \text{ cm}^{-1}$ ) corresponds to the TO phonon polariton.

A similar measurement was performed for crossing angles on the  $\Theta_o = 4.3^\circ - 15.4^\circ$  range. The obtained phonon polariton frequencies versus the  $q$  value of the excited phonons calculated according to Eq. (2) (solid symbols) and Eq. (3) (open symbols), respectively, are displayed in Fig. 3. Since in the ISRS experiments the two crossing beams are identical, for  $\mathbf{k}_L$  and  $\mathbf{k}_S$  the wave number of the spectral components having frequency larger and smaller than the mean frequency by half the polariton frequency was used in Eq. (2). The solid curve was calculated using the well-known<sup>11</sup>

$$\Omega(q) = \sqrt{\frac{\omega_{\text{LO}}^2 + \frac{q^2}{4\pi^2\epsilon}}{2}} - \sqrt{\left(\omega_{\text{LO}}^2 + \frac{q^2}{4\pi^2\epsilon}\right)^2 - \frac{4q^2\omega_{\text{TO}}^2}{4\pi^2\epsilon}}{2}} \quad (5)$$

theoretical dispersion curve of TO phonon polaritons using  $\omega_{\text{LO}} = 403 \text{ cm}^{-1}$ ,  $\omega_{\text{TO}} = 366 \text{ cm}^{-1}$ , and  $\epsilon = 9.09$ . The correctness of this curve was experimentally verified using spontaneous Raman scattering measurements.<sup>11</sup> In Fig. 3 the circles and triangles correspond to measured frequencies using a lens having 100 mm and 200 mm focal lengths, respectively, for focusing the beams. Because of the larger spot, for using lens having longer focal length the amplitude of the

ISRS signal was smaller, but at the same time the uncertainty of the  $q$  value was also smaller.

Without any doubt, the measured polariton frequencies fit to the well-known polariton dispersion curve of GaP when the  $q$  magnitude of the polariton wave vector is calculated from Eq. (2), but they definitively do not fit when  $q$  is calculated from Eq. (3). That is we proved experimentally that the wave vector of the polariton is determined by Eq. (2) even if it is excited impulsively. This result is in agreement with the principle of conservation of energy and momentum.

One consequence of our result is that Eq. (2) has to be used not only in spectral domain CARS measurements (using long light pulses) but also in temporal domain (ISRS) measurement (using shorter pulses than the temporal period of the phonon oscillation), when the two exciting beams are identical. This means that the polariton curves obtained from ISRS measurement and using Eq. (3) for the calculation of the polariton wave vector are not accurate. The inaccuracy is less significant for the smaller frequency of the created polariton relative to the central frequency of the exciting light pulse and for the lower dispersion of the investigated material at the central frequency. This is illustrated in Fig. 4, which shows for GaP and for LiTaO<sub>3</sub> the simulated dispersion curves obtainable from time domain measurements using Eq. (2) (solid lines) and Eq. (3) (dashed lines), respectively, for calculation of the momentum of the polariton. The A<sub>1</sub> TO phonon considered for LiTaO<sub>3</sub> has a frequency of 201 cm<sup>-1</sup>, while the TO phonon frequency in GaP is 403 cm<sup>-1</sup>. Furthermore, the central wavelengths of the exciting light pulses were supposed to be 610 nm and 810 nm. The smaller (polariton frequency)/(exciting frequency) ratio is the main reason for the significantly smaller difference between the curves supposing the application of Eq. (2) and Eq. (3) for LiTaO<sub>3</sub>.

Our experimental result also proves that the wave-vector diagram corresponding to Eq. (2) and shown in Fig. 1(a) is the right one. Actually, since the two beams used in an ISRS experiment have identical spectral distributions a diagram mirrored to the horizontal axis of Fig. 1(a) indicated by dashed arrows is also correct. The result is two wave vectors of the polariton directed not exactly oppositely. It is important to take this fact into account in the calculation of the expected intensity of the polariton generated for a given geometry (polarization of the excitation beams and orientation

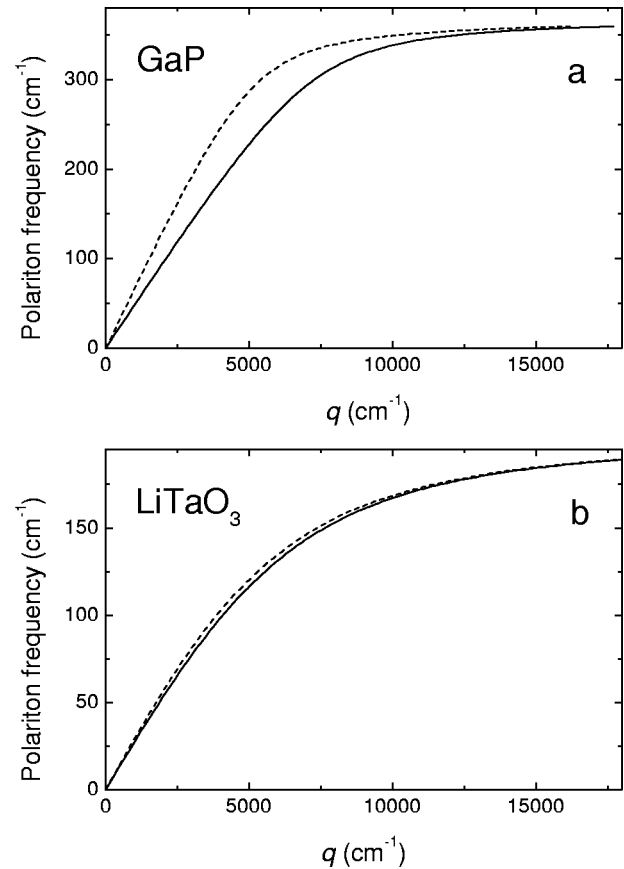


FIG. 4. Simulated dispersion curves for (a) GaP and (b) LiTaO<sub>3</sub>, obtainable from time domain measurements using Eq. (2) (solid lines) and Eq. (3) (dashed lines), respectively, for the calculation of the momentum of the polariton. In the simulation 810 nm and 610 nm central wavelengths were supposed in the case of GaP and LiTaO<sub>3</sub>, respectively.

of the investigated material). It is interesting to notice that the projection of the correctly calculated wave vectors gives the same wave vectors that are given by the incorrect calculation connected to Eq. (3). That is, the direction of diffraction (scattering) is the same irrespective of the calculation of  $q$ .

The author is grateful to A. Stepanov for taking part in the measurements.

<sup>1</sup>Y. Yan and K. A. Nelson, J. Chem. Phys. **87**, 6240 (1987).

<sup>2</sup>P. C. M. Planken, L. D. Noordam, J. T. M. Kennis, and A. Lagendijk, Phys. Rev. B **45**, 7106 (1992).

<sup>3</sup>H. J. Bakker, S. Hunsche, and H. Kurz, Phys. Rev. B **48**, 13 524 (1993).

<sup>4</sup>G. P. Wiederrecht, T. P. Dougherty, L. Dhar, K. A. Nelson, D. E. Leaird, and A. M. Weiner, Phys. Rev. B **51**, 916 (1995).

<sup>5</sup>H. J. Eichler, P. Günther, and D. W. Pohl, *Laser-Induced Dynamic Grating* (Springer, Berlin, 1986), p. 15.

<sup>6</sup>J. Etchepare, G. Grillon, A. Antonetti, J. C. Loulergue, M. D.

Fontana, and G. E. Kugel, Phys. Rev. B **41**, 12 362 (1990).

<sup>7</sup>D. P. Kien, J. C. Loulergue, and J. Etchepare, Phys. Rev. B **47**, 11 027 (1993).

<sup>8</sup>D. P. Kien, J. C. Loulergue, and J. Etchepare, Opt. Commun. **101**, 53 (1993).

<sup>9</sup>O. Albert, M. Duijser, J. C. Loulergue, and J. Etchepare, J. Opt. Soc. Am. B **13**, 29 (1996).

<sup>10</sup>H. J. Bakker, S. Hunsche, and H. Kurz, Rev. Mod. Phys. **70**, 523 (1998).

<sup>11</sup>S. Ushioda and J. D. McMullen, Solid State Commun. **11**, 299 (1972).